

1
2
3
4
5
6
7
8
9
10
11
12

This document is the unedited Author's version of a Submitted Work that was subsequently accepted for publication in *Environmental Science and Technology*, copyright © American Chemical Society after peer review. To access the final edited and published work see

<http://pubs.acs.org/articlesonrequest/AOR-jneyhAjJQIsFAmd7Bgp3>

13 C and Cl isotope fractionation of 1,2-dichloroethane
14 displays unique $\delta^{13}\text{C}/\delta^{37}\text{Cl}$ patterns for pathway
15 identification and reveals surprising C-Cl bond
16 involvement during microbial oxidation

17

18 *Jordi Palau,^{†,*} Stefan Cretnik,[‡] Orfan Shouakar-Stash,[§] Martina Höche,[‡] Martin Elsner,[‡] Daniel
19 *Hunkeler[†]**

20

21 [†]Centre for Hydrogeology and Geothermics, University of Neuchâtel, Neuchâtel, Switzerland.

22 [‡]Helmholtz Zentrum München, German Research Center for Environmental Health, Neuherberg,
23 Germany.

24 [§]Department of Earth and Environmental Sciences, University of Waterloo, Waterloo, Canada.

25

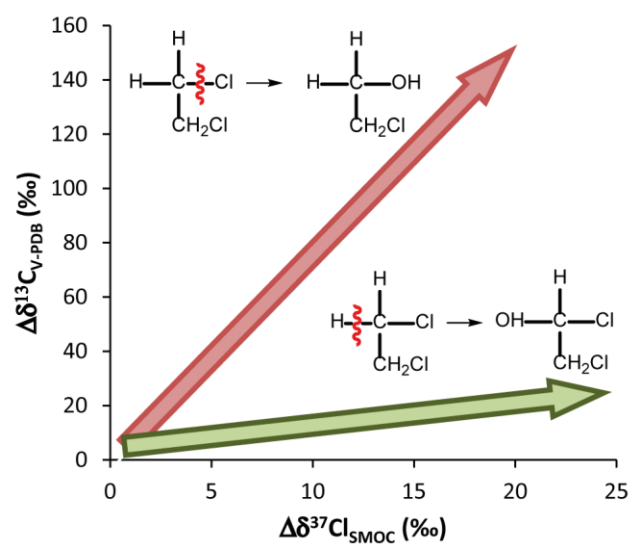
26

27

28

29

30 TOC/Abstract art
31



32
33
34
35

36 **ABSTRACT**

37 This study investigated dual element isotope fractionation during aerobic biodegradation of 1,2-
38 dichloroethane (1,2-DCA) via oxidative cleavage of a C-H bond (*Pseudomonas sp.* Strain
39 DCA1) versus C-Cl bond cleavage by S_N2 reaction (*Xanthobacter autrophicus* GJ10 and
40 *Ancylobacter aquaticus* AD20). Compound-specific chlorine isotope analysis of 1,2-DCA was
41 performed for the first time and isotope fractionation $\epsilon_{\text{bulk}}^{\text{Cl}}$ was determined by measurements of
42 the same samples in three different laboratories using two GC-IRMS and one GC-quadrupole
43 MS. Strongly pathway-dependent slopes ($\Delta\delta^{13}\text{C} / \Delta\delta^{37}\text{Cl}$), 0.78 ± 0.03 (Oxidation) and 7.7 ± 0.2
44 (S_N2), delineate the potential of the dual isotope approach to identify 1,2-DCA degradation
45 pathways in the field. In contrast to different $\epsilon_{\text{bulk}}^{\text{C}}$ values: $-3.5\pm 0.1\text{‰}$ (Oxidation), $-31.9\pm 0.7\text{‰}$
46 and $-32.0\pm 0.9\text{‰}$ (S_N2), the obtained $\epsilon_{\text{bulk}}^{\text{Cl}}$ values were surprisingly similar for the two pathways:
47 $-3.8\pm 0.2\text{‰}$ (Oxidation), $-4.2\pm 0.1\text{‰}$ and $-4.4\pm 0.2\text{‰}$ (S_N2). Apparent kinetic isotope effects of
48 ^{13}C -AKIE= 1.0070 ± 0.0002 (Oxidation), ^{13}C -AKIE= 1.068 ± 0.001 (S_N2) and ^{37}Cl -
49 AKIE= 1.0087 ± 0.0002 (S_N2) fell within expected ranges. In contrast, an unexpectedly large
50 secondary ^{37}Cl -AKIE of 1.0038 ± 0.0002 reveal a hitherto unrecognized involvement of C-Cl
51 bonds in microbial C-H bond oxidation. Our 2D isotope fractionation patterns enable for the first
52 time reliable 1,2-DCA degradation pathway identification in the field, which unlocks the full
53 potential of isotope applications for this important groundwater contaminant.

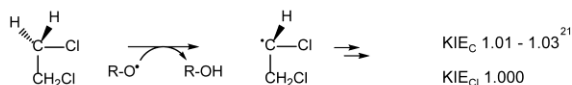
54

55 INTRODUCTION

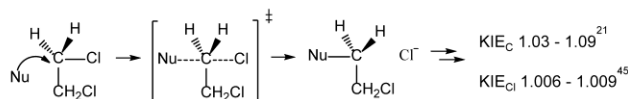
56 Chlorinated ethanes are among the most widespread contaminants in groundwater¹ and 1,2-
57 dichloroethane (1,2-DCA) has been found in 36% of 1,585 National Priorities List sites
58 identified by the United States Environmental Protection Agency (2001).² The presence of 1,2-
59 DCA - an intermediate in plastics production - in groundwater is mainly a consequence of
60 industrial activity.² A number of laboratory³⁻⁹ and field^{10, 11} studies showed 1,2-DCA
61 biodegradation under aerobic³⁻⁶ and anaerobic^{4, 7-11} conditions via different reaction pathways.⁹
62 Under aerobic conditions, 1,2-DCA can be degraded either via nucleophilic substitution (S_N2)^{5, 6}
63 or via oxidative cleavage of a C-H bond³ catalyzed by hydrolytic dehalogenase and
64 monooxygenase enzymes, respectively (Scheme 1). Initial products of both reactions, 2-
65 chloroethanol (S_N2-reaction) and 1,2-dichloroethanol (Oxidation), are further degraded to
66 ubiquitous end products, which hampers a direct identification of degradation pathways from
67 metabolite analysis. Alternative approaches to detect, and identify 1,2-DCA transformation
68 pathways in the subsurface are therefore warranted. This is crucial information in environmental
69 field studies to assess 1,2-DCA natural attenuation.

70 Scheme 1

Oxidation (C-H cleavage) (*Pseudomonas sp.* Strain DCA1) expected KIEs



S_N2-reaction (*X. autotrophicus* GJ10 and *A. aquaticus* AD20)



71

72

73 Compound specific isotope analysis (CSIA) is an innovative tool to investigate degradation
74 pathways of organic contaminants.¹²⁻¹⁴ Isotope ratios of individual compounds, measured either
75 by gas chromatography isotope ratio mass spectrometry (GC-IRMS) or GC-quadrupole mass
76 spectrometry (GC-qMS), are reported using the delta notation:

77

$$78 \quad \delta \text{ } ^h\text{E}_{\text{sample}} = \frac{R(^h\text{E}/\text{}^l\text{E})_{\text{sample}}}{R(^h\text{E}/\text{}^l\text{E})_{\text{standard}}} - 1 \quad (1)$$

79

80 where R is the isotope ratio of heavy (^hE) and light (^lE) isotopes of element E (e.g., ¹³C/¹²C and
81 ³⁷Cl/³⁵Cl). The isotope fractionation (ε) expresses by how much ^hE/^lE is smaller (negative
82 values) or larger (positive values) in the average of freshly formed products compared to the
83 substrate from which they are produced. Transformation-induced isotope fractionation is
84 generally larger than the one related to phase transfer processes such as sorption or
85 volatilization.¹⁵ Bulk (i.e. compound-average) ε values can be calculated using a modified form
86 of the Rayleigh distillation equation:

87

$$88 \quad \ln \frac{R_t}{R_0} = \ln \left(\frac{\delta \text{ } ^h\text{E}_{t+1}}{\delta \text{ } ^h\text{E}_{0+1}} \right) = \epsilon_{\text{bulk}} \cdot \ln f \quad (2)$$

89

90 where R_t and R₀ are the current and initial isotope ratios respectively, and f is the compound
91 remaining fraction.

92 Previous laboratory experiments¹⁶ showed that for 1,2-DCA different carbon ϵ_{bulk} values of -29.2
93 and -3.9‰ reflected different reaction pathways: hydrolytic dehalogenation (C-Cl bond cleavage
94 via S_N2) versus oxidation (C-H bond cleavage) respectively (Scheme 1). Knowledge of in situ
95 contaminant biodegradation reactions is essential to evaluate the fate and long term impact of
96 1,2-DCA in groundwater. For aerobic biodegradation of 1,2-DCA isotope data are particularly
97 important as no characteristic products accumulate. However, while isotope fractionation of one
98 element alone can provide pathway distinction in laboratory experiments (where mass balances
99 can be established and ϵ_{bulk} values be determined), this is not possible under field conditions.
100 Here, evidence from a second element and a dual isotope approach is necessary to distinguish
101 1,2-DCA degradation pathways.¹⁷ As observed experimentally,^{18, 19} for a given compound,
102 combined isotope analysis of two elements (e.g., $\delta^{13}\text{C}$ vs. $\delta^{37}\text{Cl}$) during the course of a reaction
103 generally yields a linear trend in a dual element isotope plot with a slope characteristic of the
104 reaction mechanism. The reason is that the dual element isotope slope ($\Lambda = \Delta\delta^{13}\text{C} / \Delta\delta^{37}\text{Cl}$,
105 where $\Delta\delta^{13}\text{C}$ and $\Delta\delta^{37}\text{Cl}$ are changes in isotope ratios during degradation) reflects isotope
106 fractionation of both elements.¹² Therefore, different slopes are expected from distinct reaction
107 pathways involving different bonds with different elements.

108 Currently, there is increasing interest in dual element isotope analysis for improved
109 differentiation of transformation mechanisms and several authors pointed out that
110 complementary mechanistic insight for 1,2-DCA aerobic biodegradation reactions could be
111 achieved by the additional analysis of chlorine¹² and/or hydrogen^{16, 20} isotope ratios. The reason
112 is that isotope fractionation can be traced back to underlying kinetic isotope effects, which are
113 highly reaction-specific.²¹ During enzymatic degradation molecules containing the light isotope
114 at the reactive site (e.g., ^{35}Cl) typically exhibit a higher reaction rate (e.g., ^{35}k) than those with a

115 heavy isotope (e.g., ^{37}Cl) resulting in a kinetic isotope effect of $\text{KIE} = k^{35} / k^{37}$.²² When a C-Cl
116 bond is broken a (primary) chlorine leaving group KIE would be expected, whereas in the
117 oxidation reaction chlorine atoms sit next to the reacting bond so that only a secondary KIE
118 would be expected (Scheme 1). Secondary isotope effects at positions next to the reacting bond
119 are generally much smaller than primary isotope effects.¹²

120 Until recently, Cl-CSIA of chlorinated aliphatic compounds was not feasible, however, because a
121 direct method that would produce a suitable Cl-containing measurement gas inside a
122 chromatographic separation gas was lacking. However, new analytical methods were developed
123 based on the measurement of selected isotopologue ions or isotopologue ion fragments in
124 unconverted analyte molecules using both continuous flow GC-IRMS²³ and GC-qMS.²⁴⁻²⁶ In
125 addition, a theoretical framework provided the theoretical justification for such evaluation of
126 isotope fractionation from ion-current ratios of molecular and fragment-ion multiplets.²⁷ A recent
127 interlaboratory study took the next step and demonstrated that comparable $\delta^{37}\text{Cl}$ values were
128 obtained when analyzing a set of pure trichlorethene (TCE) standards on eight different
129 instruments.²⁸ Since the technology is so new, however, a comparative study would also be
130 desired which shows that comparable ϵ_{Cl} values are obtained when analyzing degradation
131 samples on different instruments and in different laboratories. No such study has been conducted
132 yet. Most notably, Cl-CSIA studies have so far been applied to only few compounds, because
133 two isotopically distinct compound-specific standards are necessary for every new substance.²⁸
134 This has restricted applications primarily to chlorinated ethylenes^{18, 19, 29-34} so that - to our
135 knowledge - dual element isotope data are currently non-existent for chlorinated ethanes.

136 This study, therefore, aimed (i) to establish for the first time dual element (C & Cl) isotope
137 analysis of the chlorinated ethane 1,2-DCA; (ii) to perform the Cl isotopic analysis in three

138 different laboratories (i.e. Waterloo, München and Neuchâtel), using two different GC-IRMS
139 and one GC-qMS, in order to investigate the consistency of ϵ_{Cl} values obtained with different
140 instruments and analytical methods; (iii) to investigate carbon and chlorine isotope fractionation
141 during aerobic biodegradation of 1,2-DCA with three pure strains to determine whether the dual
142 isotope slopes are sufficiently different to potentially distinguish between hydrolytic
143 dehalogenation (S_N2) and oxidation (C-H bond cleavage) in the field.

144

145 **MATERIALS AND METHODS**

146 **Pure cultures preparation**

147 Three pure strains with known initial biotransformation mechanisms were used for the batch
148 experiments: *Pseudomonas sp.* Strain DCA1 (Oxidation), *Xanthobacter autrophicus* GJ10 and
149 *Ancylobacter aquaticus* AD20 (S_N2 reaction). *X. autrophicus* GJ10 (DSMZ 3874) and *A.*
150 *aquaticus* AD20 (DSMZ 9000) were purchased (DSMZ, Braunschweig, Germany) and
151 *Pseudomonas sp.* Strain DCA1 was kindly provided by Dr. Elizabeth Edwards (Department of
152 Chemical Engineering and Applied Chemistry, University of Toronto, Canada). The growth
153 medium was prepared as described by Hunkeler and Aravena (2000).³⁵

154 Cultures and experiments were prepared in 250 mL glass bottles, which contained 185 mL of
155 medium and were capped with Mininert-Valves (Vici Precision Sampling, Baton Rouge, LA,
156 US). Cultures were amended with 1,2-DCA (Fluka, $\geq 99.5\%$ purity) and incubated in the dark at
157 room temperature and under continuous shaking (100 rpm). Headspace 1,2-DCA concentrations
158 were monitored throughout the incubation period. Before starting the experiments the cultures

159 were transferred three times. Each subculture was spiked with pure 1,2-DCA four times before a
160 15 mL aliquot was transferred to 170 mL of autoclaved fresh medium. The spike volume was 9
161 μL of pure 1,2-DCA for the first and second subcultures and 22.5 μL for the third, leading to
162 aqueous phase concentrations of 0.6 and 1.5 mM, respectively.

163 **Experiment sampling**

164 All experiments were conducted in triplicate. Experiments and controls were amended with 22.5
165 μL of pure 1,2-DCA, corresponding to the chlorine isotopic working standard ($\delta^{37}\text{Cl}_0\text{-CHYN2} =$
166 $+0.8 \pm 0.1\text{‰}$), to produce an initial aqueous concentration of 1.5 mM. Bottles were shaken
167 upside down to prevent leakage of gas phase through the valve. After 1h of shaking, samples
168 representing the initial concentration were collected. For concentration and isotopic analysis,
169 aqueous samples (1.5 mL) were taken at selected time points and preserved frozen³⁶ in 2 mL
170 vials with NaN_3 (1 g/L). Two abiotic control bottles were prepared with 185 mL of autoclaved
171 mineral medium and samples were collected and preserved like in the experiments. For each
172 culture experiment, sample triplicates were shipped frozen to the University of Waterloo
173 (Canada) and to the Helmholtz Zentrum München (Germany) for chlorine isotope measurements.

174 **Isotopic and concentration analysis**

175 Five pure 1,2-DCA isotopic working standards, one for carbon and four for chlorine, were used
176 for instrument monitoring and external calibration of sample raw $\delta^{37}\text{Cl}$ values to the international
177 Standard Mean Ocean Chloride (SMOC) scale. The isotopic signature of the carbon standard
178 ($\delta^{13}\text{C}_{\text{V-PDB}} = -29.47 \pm 0.05\text{‰}$) was determined beforehand using an elemental analyzer coupled
179 to an IRMS. Regarding the chlorine standards, CHYN1 and CHYN2 ($\delta^{37}\text{Cl}_{\text{SMOC}} = +6.30 \pm$

180 0.06‰ and $+0.84 \pm 0.14\%$, respectively) were characterized relative to SMOC in München by
181 IRMS after conversion of 1,2-DCA to methyl chloride according to Holt et al. (1997).³⁷ IT2-
182 3001 and IT2-3002 ($\delta^{37}\text{Cl}_{\text{SMOC}} = +0.83 \pm 0.09\%$ and $-0.19 \pm 0.12\%$, respectively) were
183 calibrated against the CHYN standards using a GC-IRMS in Waterloo and a GC-qMS in
184 Neuchâtel, respectively.

185 A detailed description of analytical methods is available in the Supplementary Information (SI).
186 Carbon isotopes ratios were measured by GC-IRMS and precision based on the working standard
187 $\delta^{13}\text{C}$ value reproducibility was 0.5‰ (1 σ). Chlorine isotopic analysis was performed using the
188 following instruments: 1) Waterloo - a 6890 GC (Agilent, Santa Clara, CA, US) coupled to a
189 continuous flow IsoPrime IRMS (Micromass, Manchester, UK; currently Isoprime Ltd, UK), 2)
190 München - a TRACETM GC (Thermo Fisher Scientific, Milan, Italy) directly coupled to a
191 Finnigan MAT 253 IRMS (Thermo Fisher Scientific, Bremen, Germany) and, 3) Neuchâtel - a
192 7890A GC coupled to a 5975C quadrupole MS (Agilent, Santa Clara, CA, US). The instrument
193 used in Neuchâtel will be referred to in the following text as qMS and those used in Waterloo
194 and München as IRMS-1 and IRMS-2, respectively.

195 For analyzing 1,2-DCA, two ions of the molecular group (100, 102 m/z) were measured with the
196 IRMS-2, whereas the two most abundant fragment ions (62, 64 m/z) were used for the IRMS-1
197 and the qMS. For 1,2-DCA the intensities of the most abundant fragment ion peaks are much
198 higher than those of the parent ion peaks. Both ion couples (100, 102 and 62, 64 m/z) correspond
199 to isotopologue pairs ($[\text{}^{37}\text{Cl}\text{}^{12}\text{C}_2\text{}^1\text{H}_4]^+$, $[\text{}^{37}\text{Cl}\text{}^{35}\text{Cl}\text{}^{12}\text{C}_2\text{}^1\text{H}_4]^+$ and $[\text{}^{37}\text{Cl}\text{}^{12}\text{C}_2\text{}^1\text{H}_3]^+$, $[\text{}^{35}\text{Cl}\text{}^{12}\text{C}_2\text{}^1\text{H}_3]^+$,
200 respectively) that differ by one heavy chlorine isotope. The isotope ratio (R) can be obtained
201 from the ratio of these isotopologues according to eq. 3,²⁷

202

$$203 \quad R = \frac{{}^{37}\text{Cl}}{{}^{35}\text{Cl}} = \frac{{}^{37}\text{p}}{{}^{35}\text{p}} = \frac{k}{(n-k+1)} \cdot \frac{{}^{37}\text{Cl}_{(k)}{}^{35}\text{Cl}_{(n-k)}}{{}^{37}\text{Cl}_{(k-1)}{}^{35}\text{Cl}_{(n-k+1)}} = 2 \cdot \frac{{}^{102}\text{I}}{{}^{100}\text{I}} = \frac{{}^{64}\text{I}}{{}^{62}\text{I}} \quad (3)$$

204

205 where ${}^{37}\text{p}$ and ${}^{35}\text{p}$ are the probabilities of encountering ${}^{37}\text{Cl}$ and ${}^{35}\text{Cl}$, n is the number of Cl atoms,
206 k is the number of ${}^{37}\text{Cl}$ isotopes, ${}^{37}\text{Cl}_{(k)}{}^{35}\text{Cl}_{(n-k)}$ and ${}^{37}\text{Cl}_{(k-1)}{}^{35}\text{Cl}_{(n-k+1)}$ represent the
207 isotopologues containing k and $(k-1)$ heavy isotopes, respectively, and “I” indicates the peak
208 intensity of each ion.

209 For the qMS, isotope ratios were calculated using eq. 3 and raw $\delta^{37}\text{Cl}$ values were determined by
210 referencing versus an external 1,2-DCA working standard according to eq. 1. In this case the
211 standard was dissolved in water and measured like the samples in the same sequence.²⁶ In IRMS-
212 1 and IRMS-2 raw $\delta^{37}\text{Cl}$ values were determined by automatic evaluation of sample’s target ion
213 peaks against the ion peaks of the 1,2-DCA monitoring gas, which was introduced by a dual inlet
214 system during each sample run providing an anchor between sample measurements.²⁸
215 Subsequently, a two point linear calibration of raw $\delta^{37}\text{Cl}$ values to SMOC scale was performed
216 in each laboratory using two external working standards, i.e. IT2(3001 and 3002) for IRMS-1
217 and CHYN(1 and 2) for IRMS-2 and qMS.²⁸ The analysis schemes applied in each laboratory are
218 available in SI. For the measurements with the qMS, samples and standards were diluted to a
219 similar concentration and each of them was measured ten times, leading to a precision (1σ) on
220 the analysis of standards of $\pm 0.3\%$. For IRMS-1 and IRMS-2 precision on the analysis of
221 standards was $\pm 0.1\%$ (1σ). The $\delta^{37}\text{Cl}$ of controls remained constant ($+0.7 \pm 0.2\%$, $n = 12$) at
222 $\delta^{37}\text{Cl}_0$ within the analytical uncertainty throughout the experiment.

223 Concentrations of 1,2-DCA were measured by headspace analysis using a TRACE™ GC-DSQII
224 MS (Thermo Fisher Scientific, Waltham, MA, US) in single ion mode (51, 62, 64, 98 and 100
225 m/z). Concentrations were determined using a five point calibration curve. The estimated total
226 relative error on analysis of external standards interspersed along the sequence was ±4%.
227 Concentrations were corrected for 1,2-DCA volatilization to the bottle headspace using Henry's
228 law and Henry coefficients.³⁸ An aqueous phase 1,2-DCA concentration decrease smaller than
229 5%, due to change of headspace to solution ratio during the experiment, was estimated. The
230 average concentration of controls remained constant throughout the experiments (1.55 ± 0.03
231 mM, $\pm 1\sigma$, $n = 12$) indicating that compound losses through the valves and caps during bottles
232 shaking and samples preservation were insignificant.

233 **Calculation of apparent kinetic isotope effects (AKIE)**

234 Kinetic isotope effects are position specific whereas ϵ_{bulk} values are calculated from compound-
235 average isotope data. Therefore, observable ϵ_{bulk} values have to be converted into apparent
236 kinetic isotope effects (AKIEs) in order to obtain information about the underlying reaction
237 mechanisms.²¹ For the calculation of AKIEs a hypothesis about the reaction mechanism, or
238 assumed reaction mechanism, is necessary. The effects of non-reacting positions within the
239 molecule, as well as of intramolecular competition, are then taken into account using eqs. 4 and
240 5,²¹ respectively,

241

$$242 \quad \epsilon_{\text{rp}} \approx \frac{n}{x} \cdot \epsilon_{\text{bulk}} \quad (4)$$

243

244
$$AKIE_{C,Cl} = \frac{1}{z \cdot \varepsilon_{rp} + 1} \quad (5)$$

245

246 where ε_{rp} is the isotopic fractionation at the reactive position, n is the number of atoms of the
 247 element considered, x is the number of reactive sites and z the number of identical reactive sites
 248 undergoing intramolecular competition. In symmetric molecules such as 1,2-DCA all atoms are
 249 in equivalent reactive positions ($n = x$) and, therefore, ε_{rp} is directly obtained from eq 2.²¹ The
 250 isotope fractionation values were quantified by least square linear regression according to eq 2
 251 without forcing the regression to the origin.³⁹ As demonstrated Elsner and Hunkeler (2008),²⁷ the
 252 Rayleigh equation (eq. 2) can also be applied to calculate the isotopic fractionation of chlorine
 253 despite the higher natural abundance of ³⁷Cl compared to ¹³C.

254

255 RESULTS AND DISCUSSION

256 Chlorine isotope fractionation values from different instruments

257

258 **Table 1.** Chlorine isotopic fractionation (ε_{bulk}^{Cl}) values from pure cultures and p-values for paired
 259 t-test between instruments used.

	n ^a	r ^{2b}	IRMS-1		IRMS-2		qMS		p-values ^d
			Average	Variance ^c	Average	Variance ^c	Average	Variance ^c	
<i>A. aquaticus</i>	3	≥0.96	-4.37	0.01	-4.32	0.02	-4.63	0.04	0.923/0.390/0.670
<i>X. autrophicus</i>	3	≥0.98	-4.343	0.005	-3.960	0.007	-4.39	0.01	0.034/0.829/0.111
<i>Pseudomonas</i> <i>sp.</i>	3	≥0.95	-4.08	0.03	-3.64	0.03	-3.650	0.007	0.085/0.249/0.946

260

261 ^a Number of replicates. ^b Correlation coefficient of least-squares regression according to eq. 2. ^c

262 The variance among triplicate experiments was determined from the variance of regression for

263 each ε_i as $s_{\varepsilon}^2 = (s_{\varepsilon_1}^2 + s_{\varepsilon_2}^2 + s_{\varepsilon_3}^2)/9$.³⁹ ^d IRMS-1 vs. IRMS-2 / IRMS-1 vs. qMS / IRMS-2 vs.

264 qMS.

265

266 Chlorine isotope fractionation values ($\varepsilon_{\text{bulk}}^{\text{Cl}}$) measured with different instruments were compared

267 in Table 1. Results show excellent regressions (i.e., $r^2 \geq 0.95$) for the data from triplicate

268 experiments when measured on the same instrument (entries in Table 1). In contrast, variation

269 was greater when data from different instruments was compared. The $\varepsilon_{\text{bulk}}^{\text{Cl}}$ values from different

270 instruments were compared using paired t-tests carried out with SigmaPlotTM. The p-values were

271 above a significant level of 0.05, with the exception of the p-value for *X. autrophicus* between

272 IRMS-1 ($\varepsilon_{\text{bulk}}^{\text{Cl}} = -4.3\%$) and IRMS-2 ($\varepsilon_{\text{bulk}}^{\text{Cl}} = -4.0\%$) (Table 1). This result indicates that, in

273 general, there is no statistically significant difference in $\varepsilon_{\text{bulk}}^{\text{Cl}}$ values at the 95% confidence level.

274 The comparison of p-values for different instrument pairs does not show systematic differences,

275 suggesting that $\varepsilon_{\text{bulk}}^{\text{Cl}}$ variation between laboratories could be in part related to minor effects

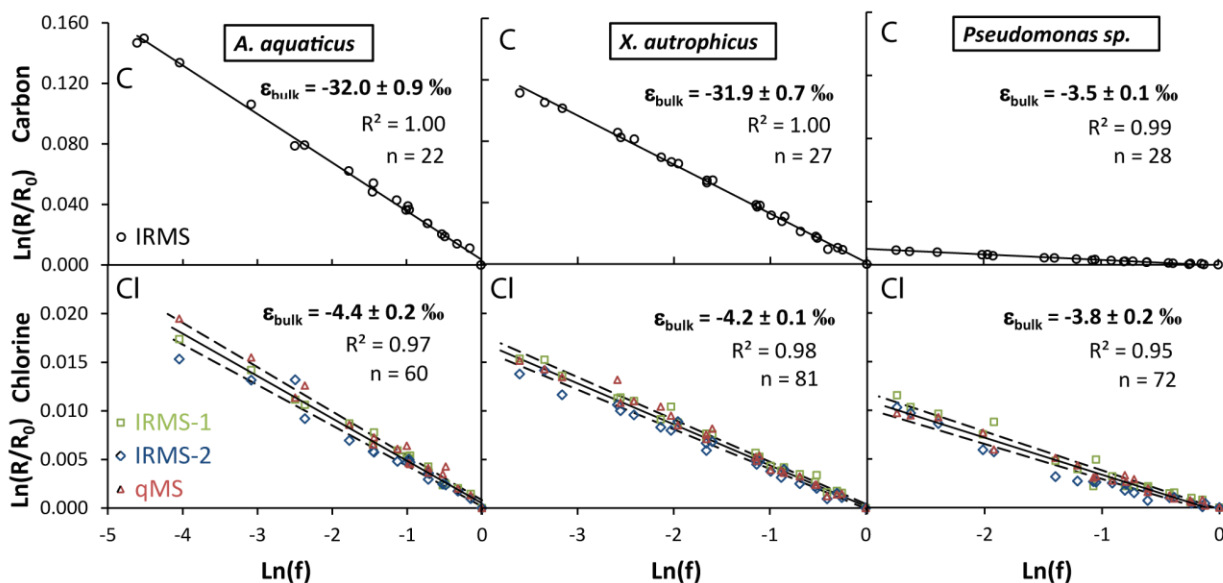
276 during sample handling. The effect of scatter in data points at late stages of reaction on

277 calculated $\varepsilon_{\text{bulk}}^{\text{Cl}}$ (Figure 1) could also explain the small differences.⁴⁰ However, removing these

278 data points did not significantly improve the agreement.

279 **C and Cl isotope fractionation and dual isotope slopes**

280



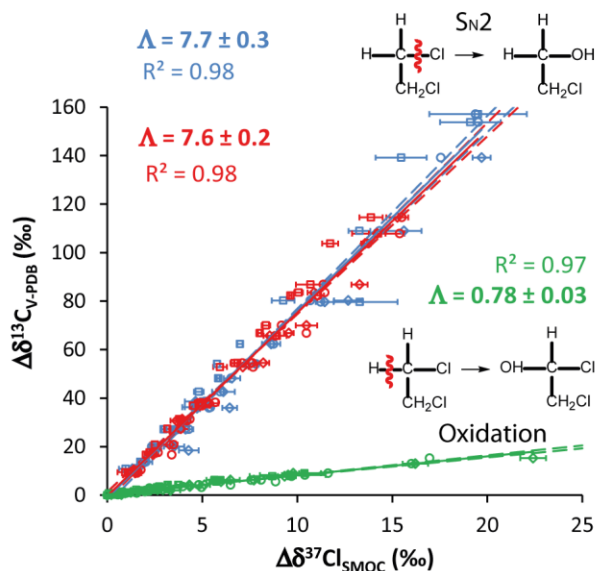
281
 282 **Figure 1.** For each culture C and Cl isotopes data from triplicate experiments were combined in
 283 Rayleigh plots. For chlorine, isotope data from different instruments were also combined. The
 284 uncertainty for the carbon and chlorine ϵ values corresponds to the $\pm 95\%$ confidence interval
 285 calculated from standard deviation of regression slope. For chlorine, dashed lines represent the
 286 95% C.I. of regression parameters.

287
 288 Degradation experiments lasted between 12h (*A. aquaticus*) and 21h (*X. autrophicus*) and 1,2-
 289 DCA transformation above 90% was reached for all the replicates. Carbon and chlorine ϵ_{bulk}
 290 values ($r^2 \geq 0.95$) (Figure 1) were determined as indicated above (eq. 2). Transformation of 1,2-
 291 DCA by *A. aquaticus* and *X. autrophicus* by a haloalkane hydrolytic dehalogenase reaction
 292 resulted in a strong enrichment of ^{13}C in the remaining substrate, showing a $\delta^{13}\text{C}$ shift of
 293 approximately 98‰ at 95% degradation. The obtained $\epsilon_{\text{bulk}}^{\text{C}}$ and $\epsilon_{\text{bulk}}^{\text{Cl}}$ values for both cultures are
 294 the same within 95% confidence intervals and $\epsilon_{\text{bulk}}^{\text{C}}$ values fall within the ranges determined

295 from previous studies^{16, 35, 41} (Table 2). As compared with carbon, a lower $\epsilon_{\text{bulk}}^{\text{Cl}}$ value of
296 approximately -4.3‰ was determined for both cultures ($\epsilon_{\text{bulk}}^{\text{C}} / \epsilon_{\text{bulk}}^{\text{Cl}} = 7.4$). Degradation of 1,2-
297 DCA by *Pseudomonas sp.* Strain DCA1 in an enzymatic monooxygenase reaction resulted in a
298 smaller carbon $\epsilon_{\text{bulk}}^{\text{C}}$ (-3.5‰) compared to nucleophilic ($\text{S}_{\text{N}}2$) reaction (Figure 1). This result is
299 consistent with the previously reported value (Table 2).¹⁶ For Cl, a $\epsilon_{\text{bulk}}^{\text{Cl}}$ value close to those
300 associated with primary Cl isotopic effects was measured ($\epsilon_{\text{bulk}}^{\text{C}} / \epsilon_{\text{bulk}}^{\text{Cl}} = 0.9$). This value is
301 unusually high given that from known mechanism a secondary isotope effect is expected (see
302 further discussion in the next Section).

303 A linear relation between $\delta^{13}\text{C}$ and $\delta^{37}\text{Cl}$ was obtained for all the strains ($r^2 \geq 0.97$) and strongly
304 different slopes ($\Lambda = \Delta\delta^{13}\text{C} / \Delta\delta^{37}\text{Cl} \approx \epsilon_{\text{bulk}}^{\text{C}} / \epsilon_{\text{bulk}}^{\text{Cl}}$) were determined for the $\text{S}_{\text{N}}2$ reaction ($\Lambda =$
305 7.7 ± 0.2) and oxidation ($\Lambda = 0.78 \pm 0.03$) (Figure 2). The slopes obtained from *X. autrophicus*
306 and *A. aquaticus* degradation experiments were the same within 95% confidence intervals.
307 Therefore, the large Λ difference among the investigated reactions enables the use of a dual
308 isotope approach to identify the different pathways in the field. In contrast, a single element
309 approach based only on carbon isotope data would lead to ambiguous interpretations because a
310 certain extent of isotope fractionation (e.g. $\Delta\delta^{13}\text{C}$) could have been caused by a strongly isotope
311 fractionating reaction that has proceeded little, or a weakly isotope fractionating reaction that has
312 proceeded further (or an unknown combination of both). Unlike in lab experiments where $\epsilon_{\text{bulk}}^{\text{C}}$
313 values can be determined,¹⁶ insight into pathways would therefore be elusive in the field. The
314 starkly contrasting trends of Figure 2 show how isotopic analysis of chlorine as second element
315 can resolve this issue. The large difference between determined slopes also enables to identify if
316 both pathways occur in the field. In ideal situations, the proportion of both competing pathways

317 could be estimated based on dual isotope data.^{42, 43} A dual isotope analysis can also be helpful in
 318 microbial laboratory experiments for substantiating conclusions about prevailing mechanisms.



319
 320 **Figure 2.** Carbon and chlorine δ isotope values from triplicate experiments and all used
 321 instruments (i.e. IRMS-1, IRMS-2 and qMS) were combined in a dual isotope plot. Symbols are
 322 as follows: blue (*A. aquaticus*), red (*X. autrophicus*), green (*Pseudomonas sp.*), circles (IRMS-1),
 323 squares (IRMS-2) and diamonds (qMS). The slopes of the linear regression lines (solid lines)
 324 give the Λ values ($\pm 95\%$ C.I.) and the dashed lines correspond to the 95% confidence intervals.
 325 Error bars of $\delta^{13}\text{C}$ values are smaller than the symbols.

326

327 **Interpretation of ^{13}C - and ^{37}Cl -AKIEs for oxidation and $\text{S}_{\text{N}}2$ -type reactions**

328

329 **Table 2.** Measured carbon and chlorine isotopic fractionation values (in ‰) and apparent kinetic
 330 isotopic effects.

	Reaction mechanism	Observed				Reported
		$\epsilon_{\text{bulk}}^{\text{C}}$ ^a	¹³ C-AKIE ^b	$\epsilon_{\text{bulk}}^{\text{Cl}}$ ^a	³⁷ Cl-AKIE ^b	$\epsilon_{\text{bulk}}^{\text{C}}$
<i>A. aquaticus</i>	S _N 2	-32.0 ± 0.9	1.068 ± 0.002	-4.4 ± 0.2	1.0089 ± 0.0004	-31.9 to -32.4 ¹⁶
<i>X. autrophiicus</i>	S _N 2	-31.9 ± 0.7	1.068 ± 0.002	-4.2 ± 0.1	1.0085 ± 0.0002	-28.7 to -33.0 ^{16, 35, 41}
<i>Pseudomonas</i> <i>sp.</i>	C-H bond cleavage	-3.5 ± 0.1	1.0070 ± 0.0002	-3.8 ± 0.2	1.0038 ± 0.0002	-3.0 ± 0.2 ¹⁶

331

332 ^a See Rayleigh plots in Figure 1. The uncertainty corresponds to the 95% confidence interval
 333 calculated from standard deviation of regression slope. ^b Calculated according eq. 5. The
 334 uncertainty was estimated by error propagation.

335

336 Hydrolytic dehalogenation (S_N2) reaction

337 Determined ϵ_{bulk} values were used to estimate the AKIEs (Table 2) according to eq. 5, which
 338 assumes that secondary isotopic effects can be neglected. For S_N2 reaction, ¹³C-AKIEs were
 339 calculated using $z = 2$ since both C-Cl bonds compete for reaction. ¹³C-AKIEs agreed well with
 340 the typical ¹³C-KIE range for a S_N2 reaction (1.03 – 1.09)²¹ (Scheme 1). Abe et al. (2009)⁴¹
 341 determined the ¹³C-AKIE of 1,2-DCA in batch degradation experiments prepared with cell free
 342 extract from *X. autrophiicus* GJ10. These authors obtained an average value (1.0597) close to the
 343 ¹³C-AKIE observed in this study (1.068), suggesting that there was no significant masking of the
 344 intrinsic KIE during compound transport thorough the cell membrane. This conclusion is in

345 agreement with the Streitwieser limit for ^{13}C -KIE in C-Cl bonds (1.057),⁴⁴ and could explain in
346 part the relatively narrow range of reported $\epsilon_{\text{bulk}}^{\text{C}}$ values (from -28.7 to -33.0‰) for both pure
347 cultures using the haloalkane hydrolytic dehalogenase reaction (Table 2). Hirschorn et al. (2007)⁹
348 measured a similar ^{13}C -AKIE (1.05) for 1,2-DCA in laboratory biodegradation experiments
349 under nitrate reducing conditions by an enrichment culture from a contaminated site, which was
350 interpreted as transformation via hydrolytic dehalogenation.

351 Similarly to carbon isotope effects, ^{37}Cl -AKIE were obtained from eq. 5 with $z = 2$. The
352 calculated ^{37}Cl -AKIE (1.009) corresponded well to the typical ^{37}Cl -KIE range for a $\text{S}_{\text{N}}2$ reaction
353 but very close to the upper end (1.006-1.009)⁴⁵ (Scheme 1). However, the ^{37}Cl -AKIE measured
354 in this study is above the theoretical primary isotope effect for 1,2-DCA enzymatic
355 dehalogenation reported by Lewandowicz et al. (2001) (^{37}Cl -KIE = 1.0065).⁴⁶ These authors also
356 measured experimentally the leaving group ^{37}Cl -AKIE for 1,2-DCA (1.0045) and 1-chlorobutane
357 (1.0066) dechlorination catalyzed by haloalkane hydrolytic dehalogenase (extracted from *X.*
358 *autrophicus* GJ10). In this former study the experimental ^{37}Cl -AKIE was determined by the
359 isotopic analysis of the released Cl^- during 1,2-DCA dechlorination and, therefore, it represents
360 the primary ^{37}Cl -AKIE. According to Lewandowicz et al. (2001)⁴⁶ and Paneth (2003)⁴⁷ an
361 explanation for the lower ^{37}Cl -AKIE of 1,2-DCA compared to 1-chlorobutane could be that the
362 dehalogenation step is reversible and the hydrolysis of the enzyme-bound intermediate is
363 responsible for the overall irreversibility of the reaction. In addition, in a recent study that
364 investigated 1,1-dichloroethane and 1,1,1-trichloroethane biodegradation by whole cell and cell
365 free extract systems,⁴⁸ ^{13}C -AKIEs for both chlorinated ethanes during degradation by cell free
366 extracts were unexpectedly lower than those determined in whole cell experiments. The higher
367 ^{37}Cl -AKIE of 1.009 compared to the theoretical primary ^{37}Cl -KIE could be explained by the

368 contribution of a β -secondary isotopic effect given that, in our study, the $^{37}\text{Cl} / ^{35}\text{Cl}$ ratios were
369 measured in the remaining 1,2-DCA and, secondary isotopic effects were neglected in the
370 primary AKIE calculation (eq. 5). The magnitude of the β -secondary ^{37}Cl -KIE can be estimated
371 from the average of KIE_i in both Cl molecular positions according to eq. 6.¹²

372

$$373 \quad \varepsilon_{\text{bulk}}^{\text{Cl}} \approx \frac{1}{2} \cdot \left(\frac{1}{\text{KIE}_{\text{primary}}^{\text{Cl}}} + \frac{1}{\text{KIE}_{\text{secondary}}^{\text{Cl}}} \right) - 1 \quad (6)$$

374

375 Plugging in the $\varepsilon_{\text{bulk}}^{\text{Cl}}$ value measured in our study (-4.3 ‰) and the reported theoretical primary
376 Cl isotopic effect of 1.0065,^{46, 47} a β -secondary ^{37}Cl -KIE of 1.0021 was estimated. Equation 6
377 assumes that $\varepsilon_{\text{bulk}}^{\text{Cl}}$ is not significantly masked by non-fractionating rate limiting processes
378 preceding the reaction step. This is a likely assumption in our case judging by the relatively high
379 carbon and chlorine AKIEs (see discussion above and Table 2). Secondary ^{13}C -KIEs are
380 generally much smaller than primary isotope effects and, therefore, they are usually omitted in
381 ^{13}C -AKIE calculations.²¹ However, for chlorine, secondary KIEs as large as primary isotope
382 effects have been recently determined theoretically during $\text{S}_{\text{N}}2$ reactions that proceed with
383 chlorine transfer between two heavy atoms.⁴⁵ In addition, in a recent experimental study that
384 investigates TCE multi-isotope fractionation during biotic reductive dechlorination,³² daughter
385 products depleted in ^{37}Cl relative to their immediate parent compounds were interpreted as
386 evidence of significant secondary Cl effects related to nucleophilic substitution reaction. The
387 conclusions of these recent studies^{32, 45} support the hypothesis that large β -secondary ^{37}Cl -KIE
388 occurs during this study.

389 Oxidative C-H bond cleavage

390 As in the hydrolytic reaction, during oxidation both C atoms also compete for reaction and thus
391 the ^{13}C -AKIE was calculated using $z = 2$ in eq. 5 (Table 2). The obtained ^{13}C -AKIE agrees well
392 with the typical ^{13}C -KIE for C-H bond cleavage (1.01 – 1.03)²¹ (Scheme 1). Primary ^{13}C -KIEs
393 generally increase with increasing mass of the bonding partner (i.e. $^{13}\text{C}\text{-KIE}_{\text{C-H}} < ^{13}\text{C}\text{-KIE}_{\text{C-Cl}}$).²¹
394 For Cl, the unexpectedly high $\epsilon_{\text{bulk}}^{\text{Cl}}$ suggests the contribution of secondary ^{37}Cl -KIEs from both
395 Cl atoms. In the absence of primary chlorine isotopic effect, the secondary ^{37}Cl -AKIE can also
396 be evaluated using eq. 5. In this case $z = 1$ since no specific bond containing Cl is broken and
397 there is, therefore, no intramolecular competition for this bond. The resultant secondary ^{37}Cl -
398 AKIE (1.004) represents the average secondary isotope effect of all positions. This result
399 supports the large β -secondary ^{37}Cl -KIE estimated above for the nucleophilic reaction. This
400 finding suggests that significant secondary ^{37}Cl -KIEs are also associated with enzymatic
401 oxidation via C-H bond cleavage. Until now, oxidative cleavage of a C-H bond has been
402 believed to affect primarily the C-H bond and to leave chlorine substituents largely unchanged.
403 This common assumption is challenged by the observed large chlorine isotope fractionation in C-
404 H bond cleavage, where involvement of a C-Cl bond would not be expected. This indicates an
405 intriguing role of the chlorine atoms which still remain to be resolved. Hypothetical contribution
406 of chlorine isotope fractionation during binding of 1,2-DCA molecules to the enzyme could be
407 an additional explanation.

408 Further insight can possibly be obtained in future studies that address $^2\text{H} / ^1\text{H}$ isotope analysis.
409 Recently, Shouakar-Stash and Drimmie (2013)⁴⁹ developed an online methodology for H-CSIA

410 of TCE and 1,2-cis-dichloroethene, however, this analytical method is still not implemented for
411 chlorinated ethanes.

412 **Implications for application of CSIA to environmental studies**

413 One of the main applications of CSIA to field studies is the estimation of contaminant
414 biodegradation extent and rate.^{15, 44, 50} For this purpose compound specific ϵ_{bulk} values from
415 laboratory experiments are necessary. For a given compound, different ϵ_{bulk} values are generally
416 associated with distinct biodegradation pathways, which in turn are sometimes related to
417 different subsurface redox environments. Therefore, redox conditions are usually used as criteria
418 to constrain the range of reported ϵ_{bulk} values. However, for 1,2-DCA different degradation
419 pathways associated with distinct ϵ_{bulk} values may even be active under aerobic conditions. In
420 addition, the hydrolytic dehalogenation pathway of 1,2-DCA has been observed under oxygen
421 and nitrate reducing conditions alike (see above)⁹. In this context, the identification of the active
422 degradation pathway in the field is crucial to choose the appropriate ϵ_{bulk} value for quantification
423 of degradation. This study demonstrates that dual isotope slopes are strongly different for
424 nucleophilic substitution (S_N2) and oxidation (C-H bond cleavage) reactions, which opens the
425 possibility to identify them using a dual isotope approach. Following this approach isotopic data
426 from the field site can be directly and intuitively interpreted.

427 Significant secondary chlorine isotopic effects were determined for the investigated reactions.
428 These results indicate that primary ^{37}Cl -AKIEs derived from CSIA could be higher than reported
429 primary ^{37}Cl -KIEs (e.g. from computational studies) if secondary isotopic effects are omitted in
430 the calculations. Hence, mechanistic interpretations based on the comparison with primary ^{37}Cl -
431 KIEs should be made with caution.

432 Finally, chlorine ϵ_{bulk} values measured with three different instruments, two GC-IRMS and one
433 GC-qMS, showed a fairly good agreement varying at most by $\pm 3.8\%$ (SD of the mean). Even
434 though the agreement was not perfect these results lend confidence to the methods used and
435 encourage the application of Cl-CSIA to investigate the fate of chlorinated compounds at
436 contaminated sites. However, further research and methodological developments are still
437 required to improve Cl-CSIA data agreement between different laboratories.

438

439 ASSOCIATED CONTENT

440 **Supporting Information**

441 A detailed description of analytical methods is available. This material is available free of charge
442 via the Internet at <http://pubs.acs.org>.

443

444 AUTHOR INFORMATION

445 **Corresponding Author***

446 Jordi Palau

447 Centre d'Hydrogéologie et de Géothermie, Université de Neuchâtel, Rue Emile-Argand 11,
448 CH-2000 Neuchâtel, Switzerland

449 E-mail: jordi.palau@ub.edu

450 **Author Contributions**

451 The manuscript was written through contributions of all authors. All authors have given approval
452 to the final version of the manuscript.

453 ACKNOWLEDGEMENTS

454 **References**

455 1. Squillace, P. J.; Moran, M. J.; Lapham, W. W.; Price, C. V.; Clawges, R. M.; Zogorski, J.
456 S., Volatile Organic Compounds in Untreated Ambient Groundwater of the United States,
457 1985–1995. *Environ Sci Technol* **1999**, *33*, (23), 4176-4187.

458 2. ATSDR Toxicological Profile for 1,2-Dichloroethane.
459 <http://www.atsdr.cdc.gov/tfacts38.pdf>

460 3. Hage, J. C.; Hartmans, S., Monooxygenase-mediated 1,2-dichloroethane degradation by
461 *Pseudomonas* sp. strain DCA1. *Appl Environ Microbiol* **1999**, *65*, (6), 2466-70.

462 4. Klecka, G. M.; Carpenter, C. L.; Gonsior, S. J., Biological transformations of 1,2-
463 dichloroethane in subsurface soils and groundwater. *J Contam Hydrol* **1998**, *34*, (1-2), 139-154.

464 5. van den Wijngaard, A. J.; van der Kamp, K. W.; van der Ploeg, J.; Pries, F.; Kazemier,
465 B.; Janssen, D. B., Degradation of 1,2-dichloroethane by *Ancylobacter aquaticus* and other
466 facultative methylotrophs. *Appl Environ Microbiol* **1992**, *58*, (3), 976-83.

467 6. Janssen, D. B.; Scheper, A.; Dijkhuizen, L.; Witholt, B., Degradation of halogenated
468 aliphatic compounds by *Xanthobacter autotrophicus* GJ10. *Appl Environ Microbiol* **1985**, *49*,
469 (3), 673-7.

- 470 7. Grostern, A.; Edwards, E. A., Characterization of a Dehalobacter Coculture That
471 Dechlorinates 1,2-Dichloroethane to Ethene and Identification of the Putative Reductive
472 Dehalogenase Gene. *Appl Environ Microbiol* **2009**, *75*, (9), 2684-2693.
- 473 8. Yu, R.; Peethambaram, H. S.; Falta, R. W.; Verce, M. F.; Henderson, J. K.; Bagwell, C.
474 E.; Brigmon, R. L.; Freedman, D. L., Kinetics of 1,2-Dichloroethane and 1,2-Dibromoethane
475 Biodegradation in Anaerobic Enrichment Cultures. *Appl Environ Microbiol* **2013**, *79*, (4), 1359-
476 1367.
- 477 9. Hirschorn, S. K.; Dinglasan-Panlilio, M. J.; Edwards, E. A.; Lacrampe-Couloume, G.;
478 Sherwood Lollar, B., Isotope analysis as a natural reaction probe to determine mechanisms of
479 biodegradation of 1,2-dichloroethane. *Environ Microbiol* **2007**, *9*, (7), 1651-7.
- 480 10. Maes, A.; van Raemdonck, H.; Smith, K.; Ossieur, W.; Lebbe, L.; Verstraete, W.,
481 Transport and activity of *Desulfitobacterium dichloroeliminans* strain DCA1 during
482 bioaugmentation of 1,2-DCA-contaminated groundwater. *Environ Sci Technol* **2006**, *40*, (17),
483 5544-5552.
- 484 11. Hirschorn, S. K.; Grostern, A.; Lacrampe-Couloume, G.; Edwards, E. A.; Mackinnon, L.;
485 Repta, C.; Major, D. W.; Sherwood Lollar, B., Quantification of biotransformation of chlorinated
486 hydrocarbons in a biostimulation study: added value via stable carbon isotope analysis. *J Contam*
487 *Hydrol* **2007**, *94*, (3-4), 249-60.

- 488 12. Elsner, M., Stable isotope fractionation to investigate natural transformation mechanisms
489 of organic contaminants: principles, prospects and limitations. *J Environ Monitor* **2010**, *12*, (11),
490 2005-2031.
- 491 13. Hofstetter, T. B.; Berg, M., Assessing transformation processes of organic contaminants
492 by compound-specific stable isotope analysis. *Trac-Trend Anal Chem* **2011**, *30*, (4), 618-627.
- 493 14. Hofstetter, T. B.; Schwarzenbach, R. P.; Bernasconi, S. M., Assessing Transformation
494 Processes of Organic Compounds Using Stable Isotope Fractionation. *Environ Sci Technol* **2008**,
495 *42*, (21), 7737-7743.
- 496 15. Braeckevelt, M.; Fischer, A.; Kastner, M., Field applicability of Compound-Specific
497 Isotope Analysis (CSIA) for characterization and quantification of in situ contaminant
498 degradation in aquifers. *Appl Microbiol Biotechnol* **2012**, *94*, (6), 1401-1421.
- 499 16. Hirschorn, S. K.; Dinglasan, M. J.; Elsner, M.; Mancini, S. A.; Lacrampe-Couloume, G.;
500 Edwards, E. A.; Lollar, B. S., Pathway dependent isotopic fractionation during aerobic
501 biodegradation of 1,2-dichloroethane. *Environ Sci Technol* **2004**, *38*, (18), 4775-4781.
- 502 17. Zwank, L.; Berg, M.; Elsner, M.; Schmidt, T. C.; Schwarzenbach, R. P.; Haderlein, S. B.,
503 New evaluation scheme for two-dimensional isotope analysis to decipher biodegradation
504 processes: Application to groundwater contamination by MTBE. *Environ Sci Technol* **2005**, *39*,
505 (4), 1018-1029.

- 506 18. Abe, Y.; Aravena, R.; Zopfi, J.; Shouakar-Stash, O.; Cox, E.; Roberts, J. D.; Hunkeler,
507 D., Carbon and Chlorine Isotope Fractionation during Aerobic Oxidation and Reductive
508 Dechlorination of Vinyl Chloride and cis-1,2-Dichloroethene. *Environ Sci Technol* **2009**, *43*, (1),
509 101-107.
- 510 19. Cretnik, S.; Thoreson, K. A.; Bernstein, A.; Ebert, K.; Buchner, D.; Laskov, C.;
511 Haderlein, S.; Shouakar-Stash, O.; Kliegman, S.; McNeill, K.; Elsner, M., Reductive
512 Dechlorination of TCE by Chemical Model Systems in Comparison to Dehalogenating Bacteria:
513 Insights from Dual Element Isotope Analysis ($^{13}\text{C}/^{12}\text{C}$, $^{37}\text{Cl}/^{35}\text{Cl}$). *Environ Sci Technol* **2013**,
514 *47*, (13), 6855-6863.
- 515 20. Chartrand, M. M. G.; Hirschorn, S. K.; Lacrampe-Couloume, G.; Lollar, B. S.,
516 Compound specific hydrogen isotope analysis of 1,2-dichloroethane: potential for delineating
517 source and fate of chlorinated hydrocarbon contaminants in groundwater. *Rapid Commun Mass*
518 *Sp* **2007**, *21*, (12), 1841-1847.
- 519 21. Elsner, M.; Zwank, L.; Hunkeler, D.; Schwarzenbach, R. P., A new concept linking
520 observable stable isotope fractionation to transformation pathways of organic pollutants. *Environ*
521 *Sci Technol* **2005**, *39*, (18), 6896-6916.
- 522 22. Bigeleisen, J.; Wolfsberg, M., Theoretical and Experimental Aspects of Isotope Effects in
523 Chemical Kinetics. *Adv Chem Phys* **1958**, *1*, 15-76.

- 524 23. Shouakar-Stash, O.; Drimmie, R. J.; Zhang, M.; Frape, S. K., Compound-specific
525 chlorine isotope ratios of TCE, PCE and DCE isomers by direct injection using CF-IRMS. *Appl*
526 *Geochem* **2006**, *21*, (5), 766-781.
- 527 24. Sakaguchi-Soder, K.; Jager, J.; Grund, H.; Matthaus, F.; Schuth, C., Monitoring and
528 evaluation of dechlorination processes using compound-specific chlorine isotope analysis. *Rapid*
529 *Commun Mass Sp* **2007**, *21*, (18), 3077-3084.
- 530 25. Jin, B.; Laskov, C.; Rolle, M.; Haderlein, S. B., Chlorine isotope analysis of organic
531 contaminants using GC-qMS: method optimization and comparison of different evaluation
532 schemes. *Environ Sci Technol* **2011**, *45*, (12), 5279-86.
- 533 26. Aeppli, C.; Holmstrand, H.; Andersson, P.; Gustafsson, O., Direct Compound-Specific
534 Stable Chlorine Isotope Analysis of Organic Compounds with Quadrupole GC/MS Using
535 Standard Isotope Bracketing. *Anal Chem* **2010**, *82*, (1), 420-426.
- 536 27. Elsner, M.; Hunkeler, D., Evaluating chlorine isotope effects from isotope ratios and
537 mass spectra of polychlorinated molecules. *Anal Chem* **2008**, *80*, (12), 4731-4740.
- 538 28. Bernstein, A.; Shouakar-Stash, O.; Ebert, K.; Laskov, C.; Hunkeler, D.; Jeannotat, S.;
539 Sakaguchi-Soder, K.; Laaks, J.; Jochmann, M. A.; Cretnik, S.; Jager, J.; Haderlein, S. B.;
540 Schmidt, T. C.; Aravena, R.; Elsner, M., Compound-Specific Chlorine Isotope Analysis: A
541 Comparison of Gas Chromatography/Isotope Ratio Mass Spectrometry and Gas

- 542 Chromatography/Quadrupole Mass Spectrometry Methods in an Interlaboratory Study. *Anal*
543 *Chem* **2011**, *83*, (20), 7624-7634.
- 544 29. Wiegert, C.; Mandalakis, M.; Knowles, T.; Polymenakou, P. N.; Aeppli, C.;
545 Macháčková, J.; Holmstrand, H.; Evershed, R. P.; Pancost, R. D.; Gustafsson, Ö., Carbon and
546 Chlorine Isotope Fractionation During Microbial Degradation of Tetra- and Trichloroethene.
547 *Environ Sci Technol* **2013**, *47*, (12), 6449-6456.
- 548 30. Wiegert, C.; Aeppli, C.; Knowles, T.; Holmstrand, H.; Evershed, R.; Pancost, R. D.;
549 Machackova, J.; Gustafsson, O., Dual Carbon-Chlorine Stable Isotope Investigation of Sources
550 and Fate of Chlorinated Ethenes in Contaminated Groundwater. *Environ Sci Technol* **2012**.
- 551 31. Hunkeler, D.; Abe, Y.; Broholm, M. M.; Jeannotat, S.; Westergaard, C.; Jacobsen, C. S.;
552 Aravena, R.; Bjerg, P. L., Assessing chlorinated ethene degradation in a large scale contaminant
553 plume by dual carbon-chlorine isotope analysis and quantitative PCR. *J Contam Hydrol* **2011**,
554 *119*, (1-4), 69-79.
- 555 32. Kuder, T.; van Breukelen, B. M.; Vanderford, M.; Philp, P., 3D-CSIA: Carbon, Chlorine,
556 and Hydrogen Isotope Fractionation in Transformation of TCE to Ethene by a Dehalococcoides
557 Culture. *Environ Sci Technol* **2013**.
- 558 33. Palau, J.; Marchesi, M.; Chambon, J. C.; Aravena, R.; Canals, A.; Binning, P. J.; Bjerg,
559 P. L.; Otero, N.; Soler, A., Multi-isotope (carbon and chlorine) analysis for fingerprinting and

- 560 site characterization at a fractured bedrock aquifer contaminated by chlorinated ethenes. *Sci*
561 *Total Environ* **2014**, 475C, 61-70.
- 562 34. Lojkasek-Lima, P.; Aravena, R.; Parker, B. L.; Cherry, J. A., Fingerprinting TCE in a
563 Bedrock Aquifer Using Compound-Specific Isotope Analysis. *Ground Water* **2012**, 50, (5), 754-
564 764.
- 565 35. Hunkeler, D.; Aravena, R., Evidence of substantial carbon isotope fractionation among
566 substrate, inorganic carbon, and biomass during aerobic mineralization of 1, 2-dichloroethane by
567 *Xanthobacter autotrophicus*. *Appl Environ Microbiol* **2000**, 66, (11), 4870-6.
- 568 36. Elsner, M.; Couloume, G. L.; Lollar, B. S., Freezing to preserve groundwater samples
569 and improve headspace quantification limits of water-soluble organic contaminants for carbon
570 isotope analysis. *Anal Chem* **2006**, 78, (21), 7528-7534.
- 571 37. Holt, B. D.; Sturchio, N. C.; Abrajano, T. A.; Heraty, L. J., Conversion of chlorinated
572 volatile organic compounds to carbon dioxide and methyl chloride for isotopic analysis of carbon
573 and chlorine. *Anal Chem* **1997**, 69, (14), 2727-2733.
- 574 38. Staudinger, J.; Roberts, P. V., A critical compilation of Henry's law constant temperature
575 dependence relations for organic compounds in dilute aqueous solutions. *Chemosphere* **2001**, 44,
576 (4), 561-576.

- 577 39. Scott, K. M.; Lu, X.; Cavanaugh, C. M.; Liu, J. S., Optimal methods for estimating
578 kinetic isotope effects from different forms of the Rayleigh distillation equation. *Geochim*
579 *Cosmochim Ac* **2004**, *68*, (3), 433-442.
- 580 40. Mundle, S. O. C.; Vandersteen, A. A.; Lacrampe-Couloume, G.; Kluger, R.; Lollar, B. S.,
581 Pressure-monitored headspace analysis combined with compound-specific isotope analysis to
582 measure isotope fractionation in gas-producing reactions. *Rapid Commun Mass Sp* **2013**, *27*,
583 (15), 1778-1784.
- 584 41. Abe, Y.; Zopfi, J.; Hunkeler, D., Effect of molecule size on carbon isotope fractionation
585 during biodegradation of chlorinated alkanes by *Xanthobacter autotrophicus* GJ10. *Isotopes*
586 *Environ Health Stud* **2009**, *45*, (1), 18-26.
- 587 42. van Breukelen, B. M., Extending the Rayleigh equation to allow competing isotope
588 fractionating pathways to improve quantification of biodegradation. *Environ Sci Technol* **2007**,
589 *41*, (11), 4004-10.
- 590 43. Centler, F.; Hesse, F.; Thullner, M., Estimating pathway-specific contributions to
591 biodegradation in aquifers based on dual isotope analysis: Theoretical analysis and reactive
592 transport simulations. *J Contam Hydrol* **2013**, *152*, 97-116.
- 593 44. Aelion, C. M.; Hohöner, P.; Hunkeler, D.; Aravena, R., *Environmental isotopes in*
594 *biodegradation and bioremediation*. CRC Press: Boca Raton, 2010; p xiv, 450 p.

- 595 45. Swiderek, K.; Paneth, P., Extending Limits of Chlorine Kinetic Isotope Effects. *J Org*
596 *Chem* **2012**, *77*, (11), 5120-5124.
- 597 46. Lewandowicz, A.; Rudzinski, J.; Tronstad, L.; Widersten, M.; Ryberg, P.; Matsson, O.;
598 Paneth, P., Chlorine kinetic isotope effects on the haloalkane dehalogenase reaction. *J Am Chem*
599 *Soc* **2001**, *123*, (19), 4550-4555.
- 600 47. Paneth, P., Chlorine kinetic isotope effects on enzymatic dehalogenations. *Acc Chem Res*
601 **2003**, *36*, (2), 120-126.
- 602 48. Lollar, B. S.; Hirschorn, S.; Mundle, S. O.; Grostern, A.; Edwards, E. A.; Lacrampe-
603 Couloume, G., Insights into enzyme kinetics of chloroethane biodegradation using compound
604 specific stable isotopes. *Environ Sci Technol* **2010**, *44*, (19), 7498-503.
- 605 49. Shouakar-Stash, O.; Drimmie, R. J., Online methodology for determining compound-
606 specific hydrogen stable isotope ratios of trichloroethene and 1,2-cis-dichloroethene by
607 continuous-flow isotope ratio mass spectrometry. *Rapid Commun Mass Sp* **2013**, *27*, (12), 1335-
608 1344.
- 609 50. Thullner, M.; Centler, F.; Richnow, H. H.; Fischer, A., Quantification of organic
610 pollutant degradation in contaminated aquifers using compound specific stable isotope analysis -
611 Review of recent developments. *Org Geochem* **2012**, *42*, (12), 1440-1460.
- 612